Ionic Charge Conservation and Long-Term Steady State in the Luo–Rudy Dynamic Cell Model

Thomas J. Hund,* Jan P. Kucera,* Niels F. Otani,* and Yoram Rudy*†‡
From the Cardiac Bioelectricity Research and Training Center and Departments of *Biomedical Engineering, †Physiology & Biophysics, and ‡Medicine, Case Western Reserve University, Cleveland, Ohio 44106-7207 USA

ABSTRACT It has been postulated that cardiac cell models accounting for changes in intracellular ion concentrations violate a conservation principle, and, as a result, computed parameters (e.g., ion concentrations and transmembrane potential, V_m) drift in time, never attaining steady state. To address this issue, models have been proposed that invoke the charge conservation principle to calculate V_m from ion concentrations ("algebraic" method), rather than from transmembrane current ("differential" method). The aims of this study are to compare model behavior during prolonged periods of pacing using the algebraic and differential methods, and to address the issue of model drift. We pace the Luo–Rudy dynamic model of a cardiac ventricular cell and compare the time-dependent behavior of computed parameters using the algebraic and differential methods. When ions carried by the stimulus current are taken into account, the algebraic and differential methods yield identical results and neither shows drift in computed parameters. The present study establishes the proper pacing protocol for simulation studies of cellular behavior during long periods of rapid pacing. Such studies are essential for mechanistic understanding of arrhythmogenesis, since cells are subjected to rapid periodic stimulation during many arrhythmias.

INTRODUCTION

Mathematical models of excitable cells have undergone a remarkable evolution since Hodgkin and Huxley's pioneering work in the 1950s (Hodgkin and Huxley, 1952). The modeling paradigm established by Hodgkin and Huxley uses the total current flowing through ion channels in the membrane to determine the transmembrane potential (V_m) (Noble, 1962; McAllister et al., 1975; Beeler and Reuter, 1977; Luo and Rudy, 1991). In this paradigm, a differential equation is solved for each current and V_m. A later stage in the evolution of mathematical models has been the development of cell models that account for dynamic changes in intracellular ion concentrations (DiFrancesco and Noble, 1985; Luo and Rudy, 1994; Winslow et al., 1999). These dynamic models build upon the original paradigm by calculating not only V_m but also intracellular ion concentrations from the transmembrane ionic currents.

Although dynamic models have proven to be a useful and widely accepted tool for studying the electrophysiology and contractility of excitable cells, they face mounting concern regarding their behavior in response to prolonged periods of rapid pacing (Guan et al., 1997; Yehia et al., 1999; Endresen et al., 2000; Rappel, 2001). Specifically, drift of intracellular ion concentrations and V_m, and the existence of an infinite number of steady states, are often cited as problems with such models (Guan et al., 1997; Yehia et al., 1999). To address these concerns, models have been formulated based on the principle of charge conservation. In this formulation, the differential equation computing V_m from the transmembrane current ("differential" method) is replaced with an algebraic equation relating V_m to intracellular ion concentrations ("algebraic" method) (Varghese and Sell, 1997; Endresen et al. 2000). It has been hypothesized that this approach produces a model that is stable with respect to drift in computed parameters (ion concentrations, V_m).

In this study, we examine the phenomenon of drift in the Luo–Rudy dynamic (LRd) mathematical model of the mammalian ventricular cell during prolonged periods of pacing. We find that no drift occurs if ions carried by the stimulus current are accounted for in the calculation of intracellular ion concentrations. When the stimulus charge is included in the formulation, the differential method and the algebraic method yield identical results.

Long-term pacing studies reproduce the physiological situation in the beating heart. During many cardiac arrhythmias, cells are subjected to periodic stimulation at a fast rate over extended periods of time. Therefore, simulation studies of cellular behavior in response to long periods of rapid pacing are essential for mechanistic understanding of arrhythmogenesis. The present study demonstrates that a dynamic model of the cardiac ventricular cell can be used for such studies and establishes the correct protocol for doing so. This work has been published in abstract form (Hund et al., 2001).

Received for publication 14 June 2001 and in final form 3 August 2001.

Address reprint requests to Yoram Rudy, Director, Cardiac Bioelectricity Research and Training Center, 319 Wickenden Building, Case Western Reserve University, Cleveland, OH 44106-7207. Tel.: 216-368-4051; Fax: 216-368-8672; E-mail: yxr@po.cwru.edu.

0006-3495/01/12/3324/08 $2.00

METHODS

The differential method

The LRd mathematical model of the mammalian ventricular myocyte (Luo and Rudy, 1994; Zeng and Rudy, 1995; Faber and Rudy, 2000) is implemented in all simulations. Every time step, model equations provide the

TABLE 1 Abbreviations

AP	Action potential
APD	Action potential duration (ms)
A_{cap}	Capacitive area of membrane (cm^2)
C_m	Membrane capacitance (μF)
F	Faraday's constant, 96,485 (C/mol)
$I_{Ca,t}$	Total Ca^{2+} current through all ion channels in LRd model ($\mu A/\mu F$) $I_{Ca,t} = I_{Ca(L)} + I_{p(Ca)} + I_{Ca(T)} + I_{Ca,b}$ (Faber and Rudy, 2000)
$I_{K,t}$	Total K^+ current through all ion channels in LRd model ($\mu A/\mu F$) $I_{K,t} = I_{Kr} + I_{Ks} + I_{K1} + I_{Kp} + I_{Ca,K}$ (Faber and Rudy, 2000)
$I_{Na,t}$	Total Na^+ current through all ion channels in LRd model ($\mu A/\mu F$) $I_{Na,t} = I_{Na} + I_{Na,b} + I_{Ca,Na}$ (Faber and Rudy, 2000)
I_{leak}	Ca^{2+} leak from NSR (mM/ms)
I_{NaCa}	Na^+–Ca^{2+} exchanger ($\mu A/\mu F$)
I_{NaK}	Na^+–K^+ pump ($\mu A/\mu F$)
I_{rel}	Ca^{2+} release from JSR (mM/ms)
I_{tr}	Ca^{2+} transfer from NSR to JSR (mM/ms)
I_{up}	Ca^{2+} uptake into NSR (mM/ms)
JSR	Junctional sarcoplasmic reticulum
NSR	Network sarcoplasmic reticulum
V_{myo}	Volume of myoplasm (μL)
V_{jsr}	Volume of JSR (μL)
V_{nsr}	Volume of NSR (μL)
$[Ca^{2+}]_{i,tot}$	Intracellular concentration of bound and free Ca^{2+} (mM)
$[Ca^{2+}]_{jsr,tot}$	JSR concentration of bound and free Ca^{2+} (mM)
$[Ca^{2+}]_{nsr}$	NSR concentration of Ca^{2+} (mM)
$[K^+]_i$	Intracellular concentration of K^+ (mM)
$[Na^+]_i$	Intracellular concentration of Na^+ (mM)
∂_t	Time derivative

transmembrane currents through ion channels, pumps, and exchangers from which changes in $[K^+]_i$, $[Na^+]_i$, $[Ca^{2+}]_{i,tot}$, $[Ca^{2+}]_{jsr,tot}$, and $[Ca^{2+}]_{nsr}$ are determined as follows ($I_{K,t}$, $I_{Na,t}$, $I_{Ca,t}$ are sums of all currents in the LRd model through K^+, Na^+, Ca^{2+} channels, respectively. See Table 1 for definitions and abbreviations).

$$\partial_t[K^+]_i = -\frac{A_{cap}C_m}{V_{myo}F}[I_{K,t} - 2I_{NaK}], \quad (1)$$

$$\partial_t[Na^+]_i = -\frac{A_{cap}C_m}{V_{myo}F}[I_{Na,t} + 3I_{NaK} + 3I_{NaCa}], \quad (2)$$

$$\partial_t[Ca^{2+}]_{i,tot} = -\frac{A_{cap}C_m}{2V_{myo}F}[I_{Ca,t} - 2I_{NaCa}] - \frac{V_{nsr}}{V_{myo}}[I_{up} - I_{leak}] + \frac{V_{jsr}}{V_{myo}}I_{rel}, \quad (3)$$

$$\partial_t[Ca^{2+}]_{jsr,tot} = I_{tr} - I_{rel}, \quad (4)$$

$$\partial_t[Ca^{2+}]_{nsr} = I_{up} - I_{leak} - \frac{V_{jsr}}{V_{nsr}}I_{tr}. \quad (5)$$

In accordance with the original modeling paradigm established by Hodgkin and Huxley (1952), transmembrane currents also provide the change in V_m every time step as

$$\partial_t V_m = -(I_{K,t} + I_{Na,t} + I_{Ca,t} + I_{NaK} + I_{NaCa}). \quad (6)$$

TABLE 2 Initial conditions

$[K^+]_i$	138.9 mM
$[Na^+]_i$	11.5 mM
$[Ca^{2+}]_i$	7.83×10^{-5} mM
$[K^+]_0$	4.5 mM
$[Na^+]_0$	132 mM
$[Ca^{2+}]_0$	1.8 mM
V_m	−89 mV
$[Ca^{2+}]_{NSR}$	1.18 mM
$[Ca^{2+}]_{JSR}$	1.18 mM
C_0	150.72 mM

Eq. 6 is numerically integrated with the Forward Euler method and a time step of 5 μs

The algebraic method

V_m can be calculated directly from intracellular ion concentrations based on a charge conservation principle (Varghese and Sell, 1997; Endresen et al., 2000). To derive this formulation for the LRd model, Eqs. 1–5 are combined as

$$\frac{V_{myo}F}{A_{cap}C_m}\left(\partial_t[K^+]_i + \partial_t[Na^+]_i + 2\cdot\partial_t[Ca^{2+}]_{i,tot} + \frac{2V_{jsr}}{V_{myo}}\cdot\partial_t[Ca^{2+}]_{jsr,tot} + \frac{2V_{nsr}}{V_{myo}}\cdot\partial_t[Ca^{2+}]_{nsr}\right) \quad (7)$$
$$= -(I_{K,t} + I_{Na,t} + I_{Ca,t} + I_{NaK} + I_{NaCa})$$
$$= \partial_t V_m.$$

Eq. 7 is integrated to give the final form of the algebraic method,

$$V_m = \frac{V_{myo}F}{A_{cap}C_m}\left([K^+]_i + [Na^+]_i + 2\cdot[Ca^{2+}]_{i,tot} + \frac{2V_{jsr}}{V_{myo}}\cdot[Ca^{2+}]_{jsr,tot} + \frac{2V_{nsr}}{V_{myo}}\cdot[Ca^{2+}]_{nsr} - C_0\right), \quad (8)$$

where C_0 is a constant of integration. Endresen et al. (2000) define C_0 as the total extracellular concentration of K^+, Na^+, and Ca^{2+}. We, instead, determine C_0 by substituting initial values for the dynamic model variables in Eq. 8. Initial conditions used in this study are provided in Table 2. Eq. 8 expresses the voltage difference across a capacitor with capacitance C_m and charge proportional to the total intracellular concentration of ions.

In both the algebraic and differential methods, transmembrane currents are calculated for every time step, after which the changes in intracellular ion concentrations are determined using Eqs. 1–5. The differential method uses Eq. 6, a differential equation, to calculate V_m, whereas the algebraic method determines V_m from Eq. 8, an algebraic expression.

Pacing protocols

Two different pacing protocols are used: The first uses a voltage-pulse stimulus and the second a current stimulus. In the first protocol, the cell is paced from a resting steady state for 33 min at basic cycle lengths (BCLs) of 300 and 1000 ms. The voltage pulse depolarizes V_m to −45 mV for 0.5 ms. As will be explained below, this protocol violates conservation for both the differential and algebraic methods. At the end of the voltage pulse, the

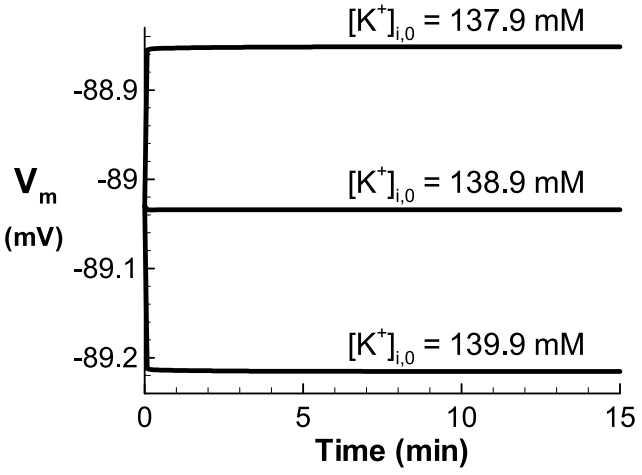

FIGURE 1 Resting V_m as a function of time before onset of pacing in the differential method. Resting steady states are shown for three different initial values of $[K^+]_i$: 137.9, 138.9, and 139.9 mM. All other initial conditions are the same for the three traces.

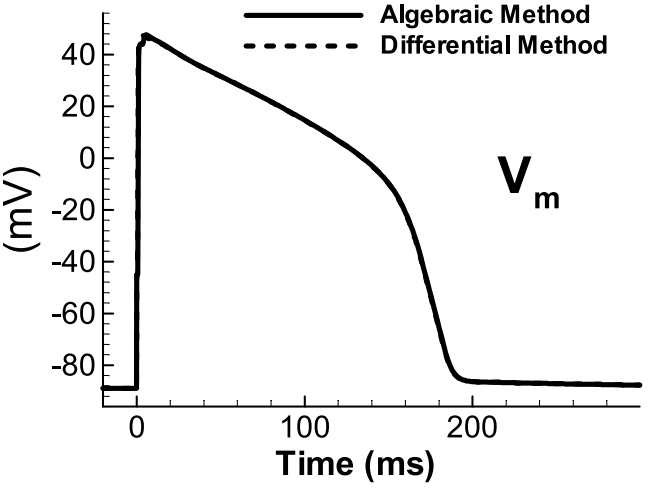

FIGURE 2 APs elicited with a voltage-pulse stimulus to −45 mV from resting steady state ($[K^+]_{i,0}$ = 138.9 mM) in the algebraic (*solid line*) and differential (*dashed line*) methods. Note that both are practically superimposed.

differential method resumes calculation of V_m using the discrete form of Eq. 6,

$$V_{m,n+1} = V_{m,n} - \Delta t(I_{K,t} + I_{Na,t} + I_{Ca,t} + I_{NaK} + I_{NaCa}), \quad (9)$$

where Δt represents the time step, and n is the time-step index. Importantly, in this scheme $V_{m,0}$ is −45 mV for computing $V_{m,1}$ after cessation of the voltage pulse. The transmembrane current initiated by the voltage-pulse stimulus continues to depolarize V_m from the holding potential of −45 mV.

The voltage pulse violates conservation in the differential method because the depolarization from the maximum diastolic potential ($V_{m,dia}$) to −45 mV is not accompanied by a consistent change in intracellular ion concentrations. In the algebraic method, conservation is violated during the voltage pulse because Eq. 8 does not hold for the original value of C_0. However, the violation is only temporary because V_m returns immediately to the value satisfying Eq. 8 for the original value of C_0 once the voltage pulse is over.

In the second protocol, the cell is paced with a current stimulus 0.5 ms in duration and −50 μA/μF in amplitude. Unless stated, the stimulus current is assumed to carry K^+ ions and is added to $I_{K,t}$ before calculation of $[K^+]_i$ using Eq. 1. This protocol insures that conservation is not violated at any time in the differential or algebraic methods. Both methods remain conservative if the stimulus current is assumed to carry Na^+ or Ca^{2+} ions, provided that the appropriate ion is accounted for in computing ion concentrations.

In dynamic model simulations as in experiments, a current stimulus is typically used to pace the cell. However, the algebraic method does not respond to a current stimulus unless an ion species is assumed as charge carrier. To compare the differential and algebraic methods in response to pacing with a nonconservative stimulus, a voltage stimulus must therefore be used. In one simulation using the differential method, the stimulus current is added to the total current in Eq. 6 but is not assumed to carry a particular ion species for the purpose of computing ion concentrations. This is done to directly demonstrate that failure to account for ions carried by the stimulus current results in drift of model parameters.

RESULTS

Before pacing, the model cell is left undisturbed for 15 min to attain a resting steady state. Figure 1 shows resting V_m as a function of time for three different initial values of $[K^+]_i$ (indicated by $[K^+]_{i,0}$) using the differential method. Initial values of all other model variables except $[K^+]_i$ are identical for all three cases. Both the differential and algebraic methods settle to the same resting steady state for each $[K^+]_{i,0}$ (V_m = −88.94 mV, −89.04 mV, −89.22 mV for $[K^+]_{i,0}$ = 137.9 mM, 138.9 mM, and 139.9 mM, respectively). A different value of $[K^+]_{i,0}$ results in a different steady state. However, once steady state is achieved (time constant to reach steady state is about 7 s), it does not drift for either the differential or algebraic methods.

Figure 2 shows the first action potential (AP) generated with a voltage-pulse stimulus from the $[K^+]_{i,0}$ = 138.9 mM resting state in Fig. 1. The algebraic and differential methods after one stimulus produce APs that are qualitatively and quantitatively very similar (error in AP duration of <0.001%). However, in Fig. 3, when the model is driven with a voltage pulse at a rapid rate (BCL = 300 ms) for a prolonged period of time, the algebraic and differential methods diverge with respect to several computed parameters, including $V_{m,dia}$, (Fig. 3 *A*), AP duration (APD, Fig. 3 *B*), $[Na^+]_i$ (Fig. 3 *C*), and $[K^+]_i$ (Fig. 3 *D*). Specifically, the computed parameters in the differential method display a linear drift that is absent in the algebraic method. Figure 4 shows that the drift of computed parameters depends on the pacing rate, with a less pronounced drift occurring when the cell is paced at a BCL of 1000 ms, consistent with previous statements in the literature (Yehia et al., 1999; Rappel, 2001).

Figure 5 shows the time-dependent behavior of computed parameters when the cell is paced with a current stimulus rather than with a voltage-pulse stimulus. Computed parameters drift if the differential method is used with a current stimulus that does not carry a particular ion species into the

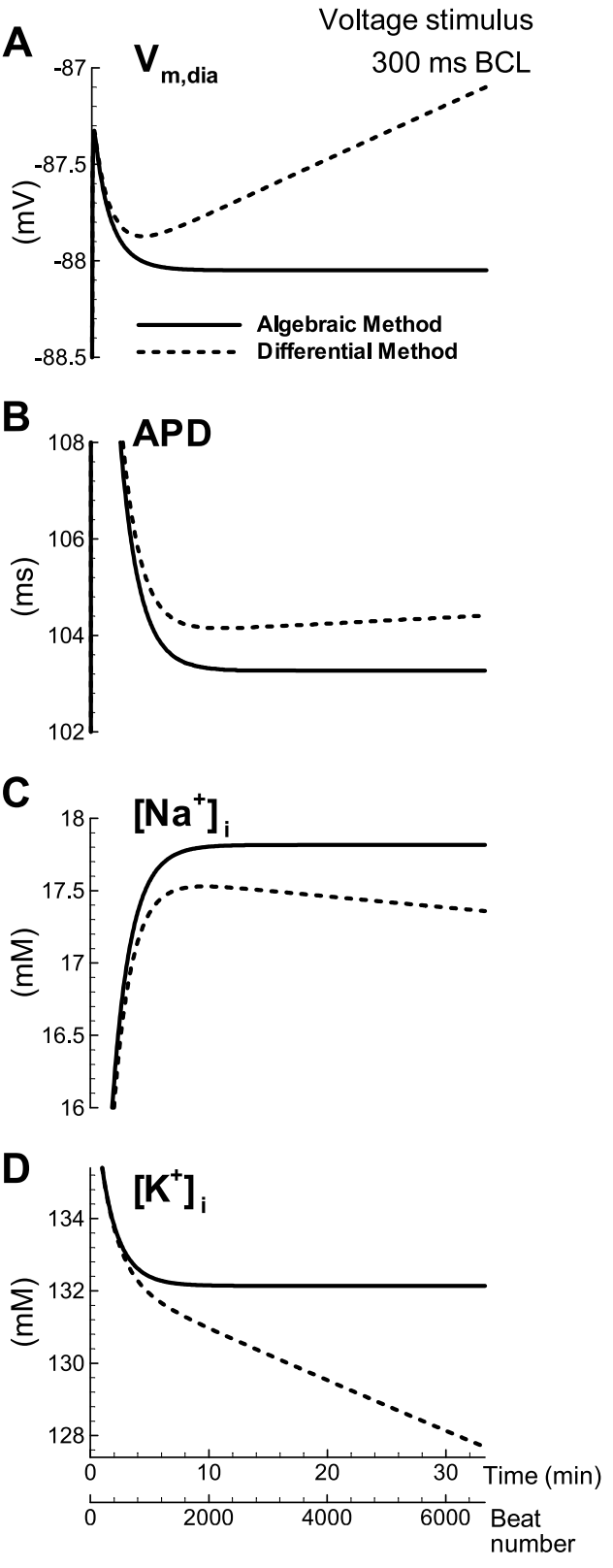

FIGURE 3 (*A*) $V_{m,dia}$, (*B*) APD, (*C*) $[Na^+]_i$, and (*D*) $[K^+]_i$ during application of a voltage pulse train at a BCL of 300 ms in the algebraic (*solid line*) and differential (*dashed line*) methods.

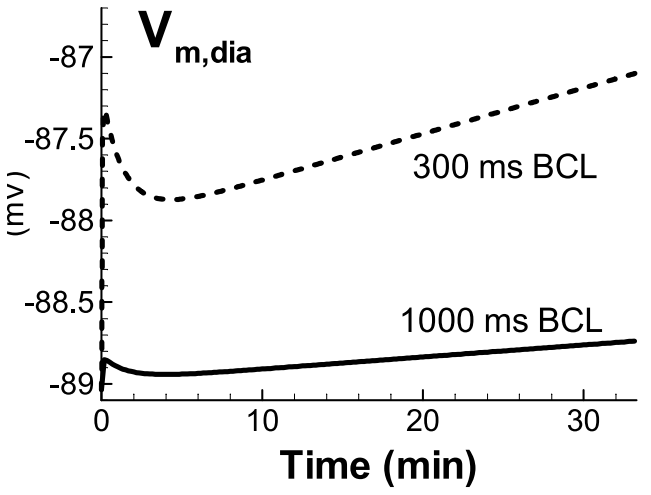

FIGURE 4 $V_{m,dia}$ during application of a voltage pulse train at two different BCLs: 300 ms (*dashed line*) and 1000 ms (*solid line*).

cell (*D.M. (no ion carrier)* in Fig. 5). Importantly, when the current stimulus is assumed to carry K^+ ions into the cell, computed parameters do not drift, and the algebraic and differential methods yield identical results. The version of the LRd model examined in this study contains a formulation of I_{NaCa} that has been modified from the original formulation to saturate at high voltages (Varghese and Sell, 1997; Faber and Rudy, 2000). When the simulation in Fig. 5 is repeated with the original formulation of I_{NaCa} (Luo and Rudy, 1994), the computed parameters again do not drift (data not shown).

Figure 6 shows $[K^+]_i$ versus V_m (phase-space plot) for nine consecutive beats during pacing at a BCL of 300 ms, after 33 min of pacing. When the model is paced with a conservative stimulus (Fig. 6 *A*), the model's trajectory in phase space adheres to a single limit cycle (limit cycles for three different $[K^+]_{i,0}$ values are shown). Figure 6 *A*, *inset* shows an enlarged limit cycle for the intermediate value of $[K^+]_{i,0}$. As V_m depolarizes during the AP upstroke, $[K^+]_i$ increases due to K^+ ions carried into the cell by the stimulus current (stage 1 in Fig. 6 *A*, *inset*). Next, K^+ ions leave the cell through K^+-selective ion channels such as the rapidly activating and slowly activating delayed rectifier K^+ currents, which contributes to the repolarization phase of the AP (stage 2). During diastole, V_m repolarizes slowly, and $[K^+]_i$ increases as I_{NaK} restores cell homeostasis by transferring Na^+ ions out of the cell and K^+ ions into the cell (stage 3). When the next stimulus is applied, the trajectory has returned to the exact point from which it began the previous cycle (*asterisk* in Fig. 6 *A*, *inset*).

In a conservative system, the entire upstroke from $V_{m,dia}$ to the AP peak is associated with a change in ion concentrations (stage 1 in Fig. 6 *A*, *inset*). However, this is not the case in the differential method when the cell is paced with a voltage-pulse stimulus (Fig. 6 *B*, shown on

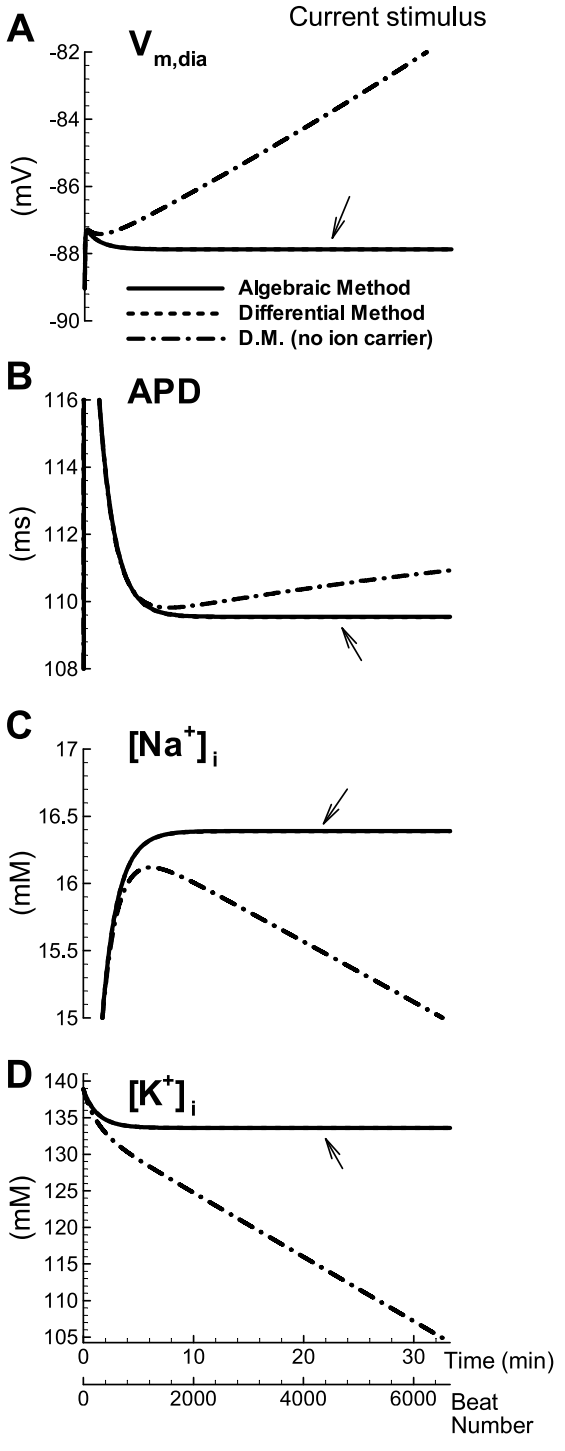

FIGURE 5 (*A*) $V_{m,dia}$, (*B*) APD, (*C*) $[Na^+]_i$, and (*D*) $[K^+]_i$ as a function of time during pacing with a current stimulus at a BCL of 300 ms using the algebraic method (*solid line*) and the differential method (*dashed line* indicated with *arrow*). In both cases, the stimulus current carries K^+ ions into the cell and contributes directly to computed changes in intracellular ion concentrations. Note the lack of drift and identical results for both methods. An additional simulation is shown using the differential method and a current stimulus that does not carry a particular ion species into the cell (*dash-dot line*). Notice that computed parameters drift if charges carried by the stimulus current are not taken into account in the computation of ion concentration changes.

the same *y* axis scale as the inset in Fig. 6 *A*). Notice that subsequent stimuli (*1*, *1′*, *1″* in Fig. 6 *B*) begin at a different point in phase space, reflecting a drift in computed parameters. As discussed in Methods, the depolarization of V_m from $V_{m,dia}$ to the holding potential of −45 mV is not associated with a parallel change in intracellular ion concentrations (stage 1 in Fig. 6 *B*, *inset*). During the voltage pulse, V_m is held constant at −45 mV and $[K^+]_i$ increases (stage 2 in Fig. 6 *B*, *inset*). Upon cessation of the voltage pulse, the Na^+ current depolarizes V_m from the already depolarized holding potential of −45 mV (stage 3 in Fig. 6 *B*, *inset*). Na^+ ions enter the cell and $[K^+]_i$ continues to increase through I_{NaK}. Importantly, entry of ions is associated with a change in V_m for only a portion of the upstroke (from −45 mV to the peak V_m of 40 mV). Fewer Na^+ ions entering the cell during the upstroke diminishes the driving force for I_{NaK}. A reduced I_{NaK} results in less entry of K^+ ions during and following the AP, which is consistent with the steady downward drift of $[K^+]_i$ between stimuli (Figs. 3 *D* and 6 *B*). Because I_{NaK} is a repolarizing current, reducing its driving force should depolarize $V_{m,dia}$ and prolong APD. This prediction is consistent with the results of Fig. 3, *A* and *B*.

The algebraic method, however, is immune to drift even when the cell is paced with a voltage-pulse stimulus (Fig. 6 *C*). Similar to the differential method, no change in ions is associated with the depolarization from $V_{m,dia}$ to −45 mV (stage 1 in Fig. 6 *C*, *inset*). Similar to the differential method, there is an increase in $[K^+]_i$ during the voltage pulse (stage 2, Fig. 6 *C*, *inset*). During this stage, Eq. 8 does not hold, and conservation is temporarily violated. However, in the algebraic method, when the voltage pulse ends, V_m returns to the value determined by Eq. 8, which is also consistent with the new intracellular ion concentrations (stage 3, Fig. 6 *C*, *inset*). From this state, the fast Na^+ current activates and depolarizes the AP upstroke to the peak V_m value of 40 mV (stage 4, Fig. 6 *C*, *inset*). It is apparent that, in the algebraic method, the change in intracellular ion concentrations during the entire upstroke from $V_{m,dia}$ to the AP peak is taken into account.

DISCUSSION

Long-term pacing is an essential protocol for the experimental and theoretical investigation of the electrophysiological properties of cardiac cells. Importantly, during many cardiac arrhythmias, cells are stimulated at a fast rate for prolonged periods of time. Under such conditions, intracellular ion concentration changes are important determinants of the cell electrophysiological behavior. Simulation studies of these processes require the use of a dynamic cell model that accounts for ion concentration changes. It is essential to insure that the model does not suffer from nonphysiological behavior during long-term pacing. In this study, we examine

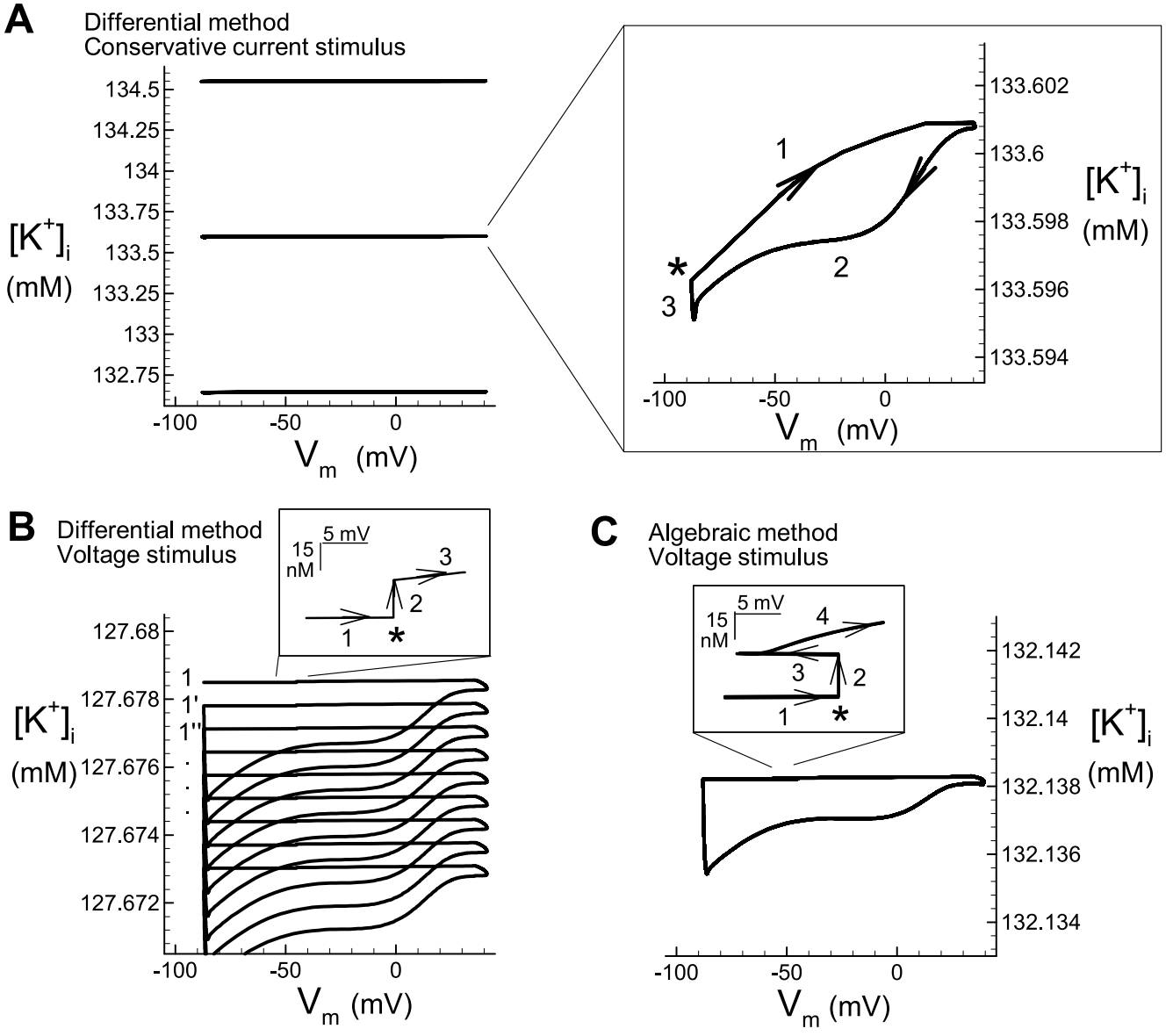

FIGURE 6 (*A*) $[K^+]_i$ as a function of V_m (phase-space plot) during pacing with a current stimulus (a conservative protocol) at a BCL of 300 ms for three different initial values of $[K^+]_i$. Enlargement of limit cycle corresponding to $[K^+]_{i,0} = 138.9$ mM is shown in the inset. The asterisk marks the application of the stimulus. (*B*) Phase-space plot during application of a voltage-pulse train (a protocol that violates conservation) using the differential method. The model's trajectory near the stimulus (*asterisk*) is enlarged in the inset. Note that, upon cessation of the voltage pulse (end of stage *2*), depolarization of V_m (stage *3*) occurs from the holding potential of −45 mV. (*C*) Same as (*B*), but using the algebraic method. Note in the inset that, upon cessation of the voltage clamp (end of stage *2*), V_m returns to a slightly repolarized value (stage *3*) before the upstroke (stage *4*).

the behavior of the LRd model during prolonged pacing protocols.

Important findings are: 1) The LRd cell model reaches a resting steady state with a time constant of ~7 s in both the differential and algebraic methods. 2) When pacing the LRd cell model, computed parameters do not drift if ions carried by the stimulus current are included when computing intracellular ion concentrations. 3) The differential and algebraic methods of calculating V_m produce identical results when the stimulus is accounted for in computing intracellular ion concentrations.

The algebraic method versus the differential method

Recently, mathematical cardiac-cell models have been formulated that replace the differential method of calculating V_m with the algebraic method (Varghese and Sell, 1997; Endresen et al., 2000). As shown in this study, the algebraic and differential methods compute identical results in a conservative system. Therefore, the choice of using the differential method over the algebraic method cannot be the fundamental reason for drift observed in such models. If

charge is conserved in the system (including charge carried by the stimulus), then the choice of method has no impact on the behavior of the system.

The researcher interested in computer modeling must choose between the two different methods for calculating V_m. The differential method solves an additional differential equation, whereas the algebraic method contains an initial condition (C_0) that must be determined before running the simulation. Both methods produce nonphysiological results when a nonconservative stimulus is used. In general, the algebraic method is more resistant to drift (Fig. 6 *C*). However, the differential method is just as robust when paced properly with a conservative stimulus (Fig. 6 *A*). Relative to the overall complexity of dynamic models, none of these distinctions is very significant in terms of implementation, and, therefore, the choice of which method to use is left to the individual researcher's discretion. Before a choice is made, however, it may be advisable to run the same simulation with both methods to ensure that conservation is not violated in the system.

Drift is caused by a nonconservative implementation of the stimulus

It has been reported in the literature that dynamic cell models, which account for changes in intracellular ion concentrations, show a nonphysiological drift in computed parameters (Yehia et al., 1999; Endresen et al., 2000; Rappel, 2001). This drift occurs during rapid pacing for prolonged periods of time (Yehia et al., 1999; Rappel, 2001). The results of the present study establish that such drift is due to a nonconservative implementation of the stimulus, and not to an intrinsic property of the LRd model. The drift disappears when ions carried by the stimulus current are accounted for in the computation of ion concentrations. In general, when using a dynamic model, any source of charge (such as the stimulus) must also be considered a source of ions. Failure to do so violates conservation and may produce a nonphysiological behavior due to drift of model parameters. In this study, the problem is easily corrected by incorporating the stimulus current into the total K^+ current in the LRd formulation. Assuming that other ions in the system (Na^+ and Ca^{2+}) to be the stimulus charge carrier is also consistent with the conservation principle, as long as these ions are accounted for in the formulation. It is worth mentioning that previous algebraic methods have been applied to automatic cells (e.g., pacemaker cells) that require no external stimulus for excitation (Varghese and Sell, 1997; Endresen et al., 2000). It would be expected, therefore, that the drift observed in the present study would not occur in such models because they do not require pacing. In addition, models that do not account for dynamic changes of intracellular ion concentrations (Hodgkin and Huxley, 1952; Noble, 1962; McAllister et al., 1975; Beeler and Reuter, 1977; Luo and Rudy, 1991) are not susceptible to the stimulus-dependent drift discussed in this study.

Another problem with dynamic models cited in the literature is that limit cycles are not unique (Guan et al., 1997; Yehia et al., 1999). Figures 1 and 6 *A* confirm that steady state in the LRd model is not unique and depends upon initial conditions. However, the existence of an infinite number of steady states is only problematic when conservation is violated (Figs. 3 and 6 *B*). Figures 4 and 6 *A* illustrate that, in a conservative system, the trajectory of the model in phase space does not stray from the limit cycle determined by the initial conditions.

Although our results suggest that a nonconservative implementation of the stimulus current underlies the reported drift in computed parameters, other possible sources of drift exist. For example, we numerically integrate Eq. 6 with the Forward Euler method, which conserves the quantity of interest (C_0 in Eq. 8). To understand the conservative nature of the Forward Euler method, we discretize Eq. 6 as

$$V_{n+1} = V_n - \Delta t \cdot \sum_j I_j, \tag{10}$$

where Δt represents the time step, and n is the time step index. Forward Euler applied to Eqs. 1–5 gives the discrete form of the ion concentration differential equations as

$$[X_j]_{n+1} = [X_j]_n - \Delta t \cdot C_m \cdot \kappa_j \cdot I_{j,n}, \tag{11}$$

where X_j is an ion species and κ_j is a constant related to the volume of distribution in the cell. We sum over ion species and combine Eqs. 10 and 11 to yield

$$V_{n+1} - \sum_j \frac{1}{C_m \cdot \kappa_j}[X_j]_{n+1} = V_n - \sum_j \frac{1}{C_m \cdot \kappa_j}[X_j]_n. \tag{12}$$

Eq. 12 shows that the quantity

$$V_n - \sum_j \frac{1}{C_m \cdot \kappa_j}[X_j]_n \equiv C_0$$

is independent of n and is thus conserved by the Forward Euler method. Numerical methods that do not conserve C_0 from one time step to the next may result in drift. For example, a method that updates I (the current) between Eqs. 10 and 11 will not conserve C_0, the result of which may be drift in computed parameters.

Simulating AP propagation in multicellular tissue models

This study emphasizes the important contribution of an external stimulus current to changes in intracellular ion concentrations during prolonged pacing of the LRd single-cell model. Microelectrodes that impale the cell for current stimulation are commonly filled with solution containing K^+ as the primary cation. This guided our choice of K^+ as

the charge carrier of the stimulus current in this study. In the heart, cells are stimulated by electrotonic current that flows through gap junctions from depolarized neighboring cells. Because K_i^+ concentration is much greater than that of other cations, it is safe to assume that K^+ is the charge carrier of this current (although anions such as Cl^- may contribute as well). Similar to the case of external current stimulation, ions carried by the intercellular electrotonic current during AP propagation should be accounted for in the calculation of intracellular ion concentrations to preserve conservation in the system. This is particularly true during fast, repetitive activation such as occurs experimentally when a multicellular tissue preparation is subject to rapid pacing, or in the in situ heart during tachyarrhythmias. For a given cell, the net ionic change (influx minus efflux) should be considered. Failure to do so may give rise to drift in computed parameters during propagation over prolonged periods of time.

It is important to note that this study examines drift in the LRd model, specifically. Nonphysiological drift has been reported in other dynamic models (Yehia et al., 1999; Michailova and McCulloch, 2001; Rappel, 2001), which should be evaluated independently for any unique sources of drift.

The authors thank Colleen Clancy, Greg Faber, and Jonathan Silva for engaging in valuable and stimulating discussions. This study was supported by grants R01-HL49054, and R37-HL33343 (to Y.R.) from the National Heart, Lung and Blood Institute, National Institutes of Health, and by a Whitaker Development Award.

REFERENCES

Beeler, G. W., and H. Reuter. 1977. Reconstruction of the action potential of ventricular myocardial fibres. *J. Physiol. (Lond.).* 268:177–210.

DiFrancesco, D., and D. Noble. 1985. A model of cardiac electrical activity incorporating ionic pumps and concentration changes. *Phil. Trans. R. Soc. Lond. B. Biol. Sci.* 307:353–398.

Endresen, L. P., K. Hall, J. S. Hoye, and J. Myrheim. 2000. A theory for the membrane potential of living cells. *Eur. Biophys. J.* 29:90–103.

Faber, G. M., and Y. Rudy. 2000. Action potential and contractility changes in $[Na^+]_i$ overloaded cardiac myocytes: a simulation study. *Biophys. J.* 78:2392–2404.

Guan, S., Q. Lu, and K. Huang. 1997. A discussion about the DiFrancesco–Noble model. *J. Theor. Biol.* 189:27–32.

Hodgkin, A. L., and A. F. Huxley. 1952. A quantitative description of membrane current and its application to conduction and excitation in nerve. *J. Physiol.* 117:500–544.

Hund, T. J., Kucera, J. P., Otani, N. F., Rudy Y. 2001. Charge conservation and steady state in the Luo–Rudy dynamic model of the cardiac cell. *Am. Biomed. Eng.* 29:5–50.

Luo, C. H., and Y. Rudy. 1991. A model of the ventricular cardiac action potential. Depolarization, repolarization, and their interaction. *Circ. Res.* 68:1501–1526.

Luo, C. H., and Y. Rudy. 1994. A dynamic model of the cardiac ventricular action potential. I. Simulations of ionic currents and concentration changes. *Circ. Res.* 74:1071–1096.

McAllister, R. E., D. Noble, and R. W. Tsien. 1975. Reconstruction of the electrical activity of cardiac Purkinje fibres. *J. Physiol. (Lond.).* 251: 1–59.

Michailova, A., and A. McCulloch. 2001. Model study of ATP and ADP buffering, transport of Ca^{2+} and Mg^{2+}, and regulation of ion pumps in ventricular myocyte. *Biophys. J.* 81:614–629.

Noble, D. 1962. A modification of the Hodgkin–Huxley equations applicable to Purkinje fibre aciton and pacemaker potential. *J. Physiol. (Lond.).* 160:317–352.

Rappel, W.-J. 2001. Filament instability and rotational anisotropy: a numerical study using detailed cardiac models. *Chaos.* 11:71–80.

Varghese, A., and G. R. Sell. 1997. A conservation principle and its effect on the formulation of Na–Ca exchanger current in cardiac cells. *J. Theor. Biol.* 189:33–40.

Winslow, R. L., J. Rice, S. Jafri, E. Marban, and B. O'Rourke. 1999. Mechanisms of altered excitation–contraction coupling in canine tachycardia-induced heart failure, II: Model studies. *Circ. Res.* 84:571–586.

Yehia, A. R., D. Jeandupeaux, F. Alonso, and M. R. Guevara. 1999. Hysteresis and bistability in the direct transition from 1:1 to 2:1 rhythm in periodically driven single ventricular cells. *Chaos.* 9:916–931.

Zeng, J., and Y. Rudy. 1995. Early afterdepolarizations in cardiac myocytes: mechanism and rate dependence. *Biophys. J.* 68:949–964.